Available online at www.sciencedirect.com
SCIENCE DIRECT®
Journal of Pharmaceutical and Biomedical Analysis
31 (2003) 299–309
JOURNAL OF PHARMACEUTICAL AND BIOMEDICAL ANALYSIS
www.elsevier.com/locate/jpba

Investigation of structure and enantioselectivity of BSA-encapsulated sol–gel columns prepared for capillary electrochromatography

Kumiko Sakai-Kato, Masaru Kato, Haruna Nakakuki, Toshimasa Toyo'oka *

Department of Analytical Chemistry, School of Pharmaceutical Sciences, University of Shizuoka, 52-1 Yada Shizuoka, Shizuoka 422-8526, Japan

Received 4 October 2002; received in revised form 13 November 2002; accepted 15 November 2002

Abstract

We have developed a protein-encapsulation technique using sol–gels for the preparation of monolithic capillary columns for capillary electrochromatography. Due to the silica-based matrix used, this hydrogel generates the appropriate electroosmotic flow. Electroosmotic mobility varied according to the gels fabricated under the different gelation conditions and using different starting materials. Using attenuated total reflectance (ATR)-FT-IR, the residual silanol groups in each hydrogels could be measured without drying procedures and it was found that electroosmotic mobility decreased with a reduction in the residual silanol groups. Enantiomeric separation of D,L-Trp was evaluated using bovine serum albumin (BSA)-encapsulated column. Preparatory conditions for BSA-encapsulated columns also influenced the retention time and enantioselectivity of D,L-Trp. The gels composed of clusters with the diameter of around 1 μm. According to ATR-FT-IR study, BSA maintained its structure after encapsulation in the gel.
© 2002 Elsevier Science B.V. All rights reserved.

Keywords: Sol–gel; Bovine serum albumin; Capillary electrochromatography; Electroosmotic flow; Enantioselectivity; Gel structure

1. Introduction

Capillary electrochromatography (CEC) has been regarded as a very promising analytical separation technique that combines the efficiency of capillary zone electrophoresis and the selectivity of liquid chromatography [1,2].

The use of monolithic columns in CEC had been shown advantageous in many ways over the conventional packed columns [3–7]. A major advantage is the ease of monolith preparation inside a capillary. An additional advantage is the fritless design of monolithic column. Bubble formation at the frit has been a serious problem for

* Corresponding author. Tel.: +81-54-264-5656; fax: +81-54-264-5593.
E-mail address: toyooka@ys2.u-shizuoka-ken.ac.jp (T. Toyo'oka).

0731-7085/02/$ - see front matter © 2002 Elsevier Science B.V. All rights reserved.
PII: S0731-7085(02)00638-6

conventional packed columns. Many monolithic columns for CEC have been fabricated using a variety on monomers, such as acrylamide [3], methacrylate [4] and alkoxysilane [5–7]. Ideally, the monomer used should contain hydrophobic groups for solute interactions as well as charged groups for the generation of electroosmotic flow (EOF). Fujimoto have developed a unique hydrogel column made of cross-linked polyacrylamide for separations of uncharged, low molecular weight compounds [8,9]. The presence of negatively-charged functional groups permits the development of EOF on the application of an electrical field.

We recently developed a novel protein-encapsulation technique using the sol–gel method for the preparation of monolithic capillary columns for capillary electrophoresis (CE) and CEC system [10–13]. Various proteins were encapsulated into tetramethoxysilane (TMOS)-based silica matrix in a singe step within a capillary. This method enabled the incorporation of various biological functions into CE or CEC system. Two proteins, bovine serum albumin (BSA) and ovomucoid were encapsulated in the silica matrix and their enantioselectivity was evaluated for the separation of some drug enantiomers [10,13]. Trypsin- and microsome-encapsulated capillary column, which was integrated into CE system, enabled the creation of an on-line enzyme reactor with enhanced reactivity and stability [11,12]. These results show that the technique presented is potentially useful for biomolecule-encapsulated micro assay systems. Because the resultant silica matrix was fabricated without drying procedures, there was no shrinkage of gel within the capillary nor loss of protein activities. The monolithic hydrogels showed excellent properties for CEC. They include high mechanical strength, penetration of flow and generation of a significant EOF. The presence of an EOF in CEC is particularly suitable for column packing.

Nevertheless, a good control and understanding of the gel structure during fabrication is essential for high quality and reproducible separations. Hence a detailed investigation will be performed in this work to characterize the structure and property of the protein encapsulated gels.

2. Experimental section

2.1. Materials and chemicals

Fused-silica capillary (75 μm i.d.) was obtained from Polymicro Technologies Inc. (Phoenix, AZ). TMOS and methacryloxypropyltrimethoxysilane (MPTMS) were purchased from Tokyo Kasei (Tokyo, Japan). BSA (crystallized cold alcohol precipitate 97%) was purchased from Wako Pure Chemicals (Osaka, Japan). Methyltrimethoxysilane (MTMS) was purchased from ShinEtsu Chemicals (Tokyo, Japan). D,L-Trp was purchased from Sigma-Aldrich (Milwaukee, WI). Water was purified by a MilliQ system (Millipore, Bedford, MA).

2.2. Monolithic capillary column preparation

The capillary column (40 cm) was pretreated with MPTMS as described in our previous reports [10], and then it was filled with a 20 mM phosphate buffer (pH 7) prior to use. The polyimide coating of the treated capillary was etched with concentrated sulfuric acid to make a detection window.

The sol–gel reaction was performed as described in our previous report [10]. The monomer solution was obtained by mixing the following reagents just prior to use: (1) 761 μl TMOS, (2) 169 μl water and (3) 11 μl 0.04 N HCl. This solution was stirred for 20 min to allow the formation of fully or partially hydrolyzed silane, $SiOH_{4-n}(OMe)_n$. Phosphate buffers of various pH and concentration with or without BSA (5% (w/v)) were then added to this monomer solution.

After mixing and ultrasonication for 5 s, the mixture solution was carefully aspirated with a 1.0-ml disposable syringe from the inlet of the capillary, which was in advance filled with 20 mM phosphate buffer (pH 7.0), until the sol plug becomes 5-cm long under the microscopic observation. The ends of the capillary were then sealed with parafilm and placed at room temperature for at least 4 days to allow the formation of the sol–gel.

After the sol–gel is formed, the capillary was cut up to adequate length for instruments. The total

length and effective length were 36 and 27 cm, respectively. The capillary was carefully installed in a CE cartridge and conditioned electrokinetically (−2 kV) with 20 mM phosphate buffer (pH 7.0) for 1 h to eliminate all the methanol or protein not encapsulated in the sol–gel matrix.

2.3. CEC equipment

CEC experiments were carried out on Hewlett Packard ^{3D}CE system (Palo Alto, CA) equipped with a diode array detector. Samples were introduced electrokinetically at the anodic side (4 kV, 5 s), and the same voltage was used for separation. The temperature was kept at 25 °C in all experiments.

All samples were prepared in the mobile phase, 20 mM phosphate buffer (pH 7.0). All solutions were filtered through a 0.22-μm membrane (Millipore) and degassed by ultrasonication.

The enantioselectivity of Trp by BSA-encapsulated column was evaluated using α' ($=t_D/t_L$), where t_D and t_L were the retention times of D-Trp and L-Trp, respectively, because of the following reasons; (1) it is hard to measure exact t_0 [14], (2) the peak shape of L-Trp was often very asymmetric owing to the strong interaction with BSA and it was difficult to calculate half width of the peak.

2.4. FT-IR measurement

To investigate the hydrogel structure, IR spectra were collected with a JASCO FT/IR-550 (JASCO, Tokyo, Japan) equipped with the attenuated total reflectance (ATR) apparatus, ATR-500/M (JASCO). The TMOS-hydrolyzed solution was added to phosphate buffer with or without BSA, and was then immediately placed into an ATR liquid cell for measurement. The cell was sealed to prevent the liquid evaporation. The FT-IR spectra were obtained at the appropriate period of time during the gelation process. The spectra obtained between 1300 and 800 cm^{-1} was fitted using Origin 5.0 J (OriginLab, MA, USA). Six Gaussian bands were obtained, which were originated from the silanol groups, methanol and siloxane structure with four different vibrational modes.

The contents of residual silanol groups were evaluated using the following equation:

$$\text{Residual silanol (\%)} = A/(A + B_1 + B_2 + B_3 + B_4)\times 100 \quad (1)$$

where A is a peak area of silanol groups at about 960 cm^{-1} (indicated by number 1 in Fig. 2) and B_1–B_4 are peak areas of four siloxane peaks derived from different vibrational modes, whose positions are at about 1075, 1160, 1200, 1240 cm^{-1} (indicated by number 3–6, respectively) with variation of the order of 20 cm^{-1} [15,16].

The BSA spectra between 1800 and 1400 cm^{-1} were obtained after subtracting the background (buffer solution) from the sample (buffer+protein), using a scaling factor that made the 1720–1800 cm^{-1} region flat [17,18].

2.5. Dynamic light scattering measurement

The diameter of the sol particles during gelation was measured at 25 °C using dynamic light scattering (DLS) measurement. An ELS-8000 (Otsuka Electric Co., Tokyo, Japan) with a 10 mW He–Ne laser with scattering angle of 90° was used. After adding 50 mM phosphate buffer (pH 5.0) with or without 5% (w/v) BSA to the TMOS (containing 10% MTMS)-hydrolyzed solution, the mixture was quickly vortexed and sonicated, and was immediately placed into a disposable cuvette. The cuvette was installed in a DLS and the measurement was immediately carried out. The data were obtained at a few minutes intervals. The average diameter was calculated by size analysis software with Cumulant analysis.

3. Results and discussion

The sol–gel reaction involves the following steps [19]: (1) the hydrolysis of alkoxysilane; (2) the condensation of hydrated silica to form siloxane bonding (Si–O–Si); and (3) the polycondensation of linkage of additional silanol group to form the cyclic oligomers. While the silicate network forms, it traps the protein molecules.

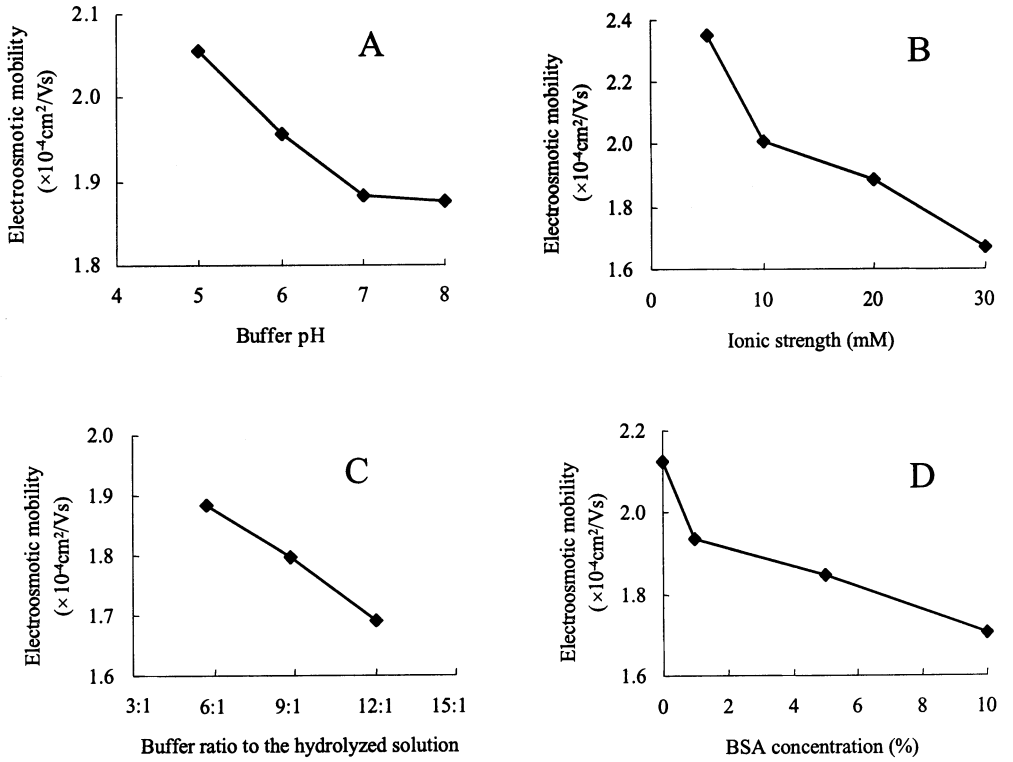

Fig. 1. Effect of gelation conditions on the electroosmotic mobility. (A) Buffer pH, (B) Ionic strength, (C) Buffer ratio to the hydrolyzed solution, (D) BSA concentration. *Conditions*: Sample: 5 mM thiourea. Mobile phase: 20 mM phosphate buffer (pH 7.0). Applied voltage: 4 kV. Injection: 4 kV, 5 s. Column length: 36 cm. Gel length: 5 cm. Detection: 254 nm.

Hydrolysis:

$$Si(OR)_4 + H_2O \rightarrow (RO)_3SiOH + ROH$$

Condensation:

$$2(RO)_3SiOH \rightarrow (RO)_3Si\text{–}O\text{–}Si(OR)_3 + H_2O$$

$$(RO)_4Si + (RO)_3SiOH \rightarrow (RO)_3Si\text{–}O\text{–}Si(OR)_3 + ROH$$

A small amount of unreacted silanols will also be present in the resultant gel, which will be responsible for generating an EOF.

3.1. Dependence of electroosmotic mobility on gelation conditions

Conditions such as pH, ionic strength, and starting materials were found to influence the gelation rate and the geometry of the resultant gel [19]. Since the magnitude of the EOF is an important characteristic of a CEC column, the effect of the gelation conditions on the EOF was investigated. Under various conditions, 5-cm long gel sections were fabricated in 75-μm capillaries. The parameters examined include buffer pH, ionic strength, ratio of buffer-to-hydrolyzed solution, and BSA concentration. The electroosmotic mobility was measured in each case using thiourea as an EOF marker [6,20]. The results were shown in Fig. 1A–D. All CEC conditions such as mobile phase, applied voltage and column length were kept constant except for the gelation condition.

To study the effect of buffer pH, the TMOS-hydrolyzed solution was mixed with 20 mM phosphate buffer at various pH values ranging 5–8. This pH range should be compatible to the encapsulated biomolecules. According to Fig. 1A, decreasing electroosmotic mobility was observed

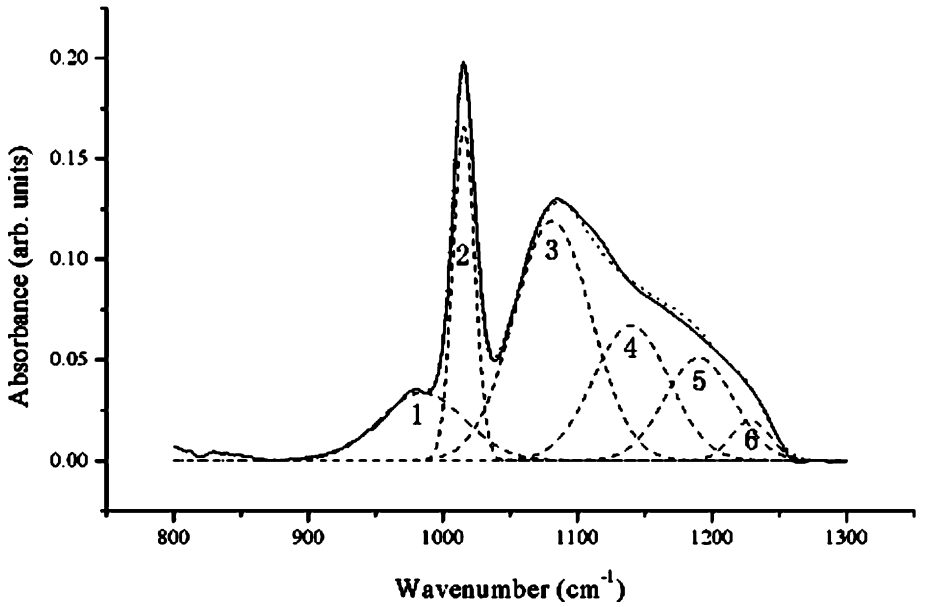

Fig. 2. Deconvolution of the IR absorption band at 800–1300 cm^{-1} of hydrogel. Solid line: experimental spectrum. Dashed line: decomposed spectrum. Dotted line: sum of the six decomposed spectra. Sample: hydrogel fabricated using 5 mM phosphate buffer.

at higher pH conditions. The column prepared at pH 8.0 showed relatively poor data, as the electroosmotic mobility was not stable. This is ascribed to the fact that silica materials are not stable above pH 8.0 [13].

Secondly, the dependence of ionic strength was examined. Phosphate buffer (pH 7.0) at concentrations ranging from 5 to 30 mM was mixed with the hydrolyzed solution and allowed to gel within a capillary. An increase in ionic strength resulted in a decrease of the electroosmotic mobility (Fig. 1B). At concentrations of 40 mM and above, significant bubble formation occurred and therefore the electroosmotic mobility could not be measured.

The volumetric ratio of phosphate buffer (20 mM, pH 7.0) to the hydrolyzed solution was varied from 6:1 to 12:1. A linear decrease in the electroosmotic mobility was observed with increasing ratio, as shown in Fig. 1C.

BSA solution at concentrations ranging from 0 to 10% (w/v) in 50 mM phosphate buffer (pH 5.0) was mixed with the hydrolyzed solution. As BSA concentration increased, the electroosmotic mobility decreased (Fig. 1D).

In CEC, the mobile phase contains an electrolyte and is transported through the capillary column by EOF. The EOF is generated at the interface between the solution and a charged surface, such as the deprotonated silica [21]. The sol–gels also possess some unreacted silanols, which are believed to be responsible for the resultant EOF. To confirm this hypothesis, the content of residual silanol groups in gels was determined and correlated to the resultant EOF. ATR-FT-IR was used to measure the silanol content. It has many advantages over the conventional method of using potassium bromide disk. ATR enables to measure silanol groups without drying the gel. Furthermore, it allows continuous measurement during the time-course of gelation.

Fig. 2 shows a typical IR spectrum of the gel in the region between 1300 and 800 cm^{-1}. The band at 960 cm^{-1}, indicated by number 1, corresponds to silanol groups. The band at 1016 cm^{-1}, indicated by number 2, corresponds to MeOH, which was generated in the process of hydrolysis and condensation. The bands indicated by 3–6 correspond to SiO_2 structure with different vibration modes [16]. The peak area of the silanol peak

gradually decreased and the peak area of SiO_2 gradually increased, as the gelation process progressed. Changes in the relative intensities ended in approximately 3 days, and thus it was concluded that the reaction was almost completed at that point. To determine the amount residual silanol groups after the reaction was completed, ATR measurements were performed on 5-day old samples under various conditions of buffer pH and ionic strength.

As shown in Fig. 3A, the residual silanol groups decreased as buffer pH of gel preparation increased. This change coincided with that of electroosmotic mobility. The residual silanol groups also decreased with an increase in the ionic strength (Fig. 3B), which is associated with the decrease in the electroosmotic mobility. These results indicate that electroosmotic mobility have close relationship with the content of residual silanol groups in gels [22]. A similar result was reported using acrylamide-gel filled capillary columns, in which the increase in negatively-charged groups in gel increased the electroosmotic mobility [8]. Therefore, EOF can be controlled by changing the gelation conditions. Of course, other factors such as mobile phase conditions largely influence electroosmotic mobility.

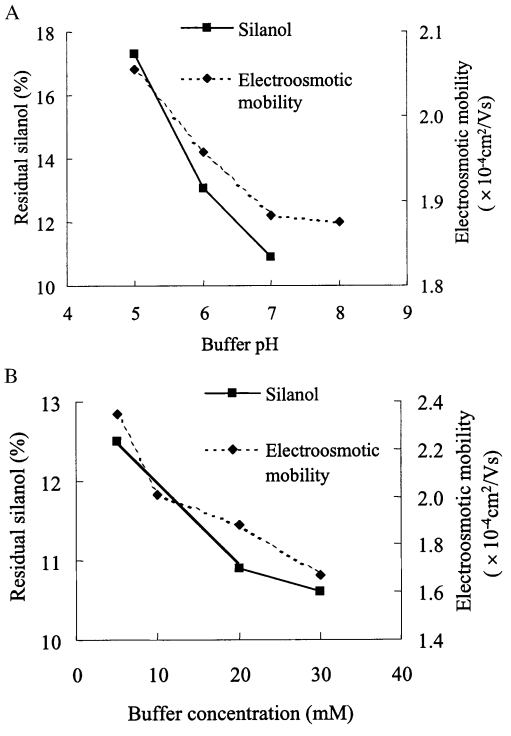

Fig. 3. Relationship between the electroosmotic mobility and the relative contents of silanol groups. CEC conditions are the same in Fig. 1.

3.2. *Enantiomeric separation of D,L-Trp by BSA-encapsulated columns*

Enantiomeric separation of D,L-Trp was evaluated using BSA-encapsulated columns prepared under different conditions. Fig. 4 shows the influence of buffer pH for gel preparations. The BSA was dissolved in phosphate buffer at pH 5, 6 and 8 and encapsulated in gel. As illustrated, increasing retention time was observed at higher

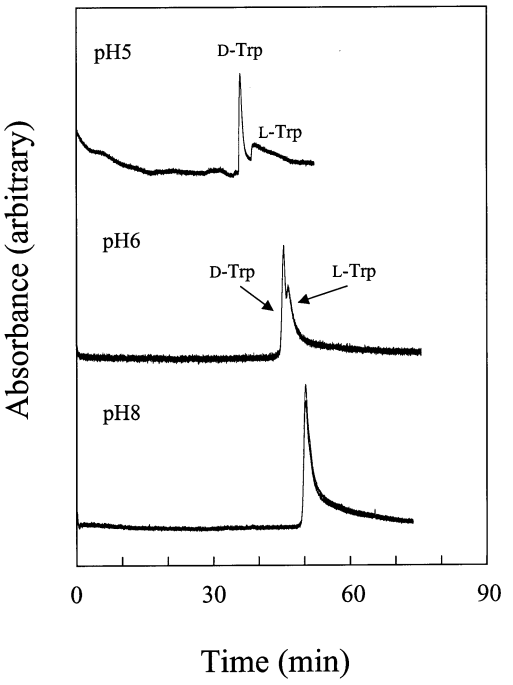

Fig. 4. Separation of D,L-Trp by BSA-encapsulated column prepared using phosphate buffer at various pH. *Conditions:* Gel composition: 5%(w/v) BSA in 20 mM phosphate buffer (pH 5-8): TMOS-hydrolyzed solution = 6:1. Sample: 5 mM D,L-Trp. Mobile phase: 20 mM phosphate buffer (pH 7.0). Applied voltage: 2 kV. Injection: 2 kV, 3 s. Column length: 36 cm. Gel length: 5 cm. Detection: 280 nm.

pH, which coincided with the result of EOF velocity shown in Fig. 1A. On the other hand, the enantioselectivity was deteriorated at pH 6 and 8. Since the isoelectric point of BSA is about 4.7, it possesses a negative charge as do the silanol groups of the gel prepared in the buffer at pH 6 and 8. Consequently, electric repulsion between BSA and gel presumably prevents the encapsulation process.

As reported in our previous paper, the content of alkoxysilane monomers also influenced the electroosmotic mobility [10]. Three different compositions of MTMS (0, 10, and 30%) to TMOS solution were used to prepare hydrolyzed solution and mixed with phosphate buffer containing BSA. Fifty millimole phosphate buffer of pH 5 was used from the results of Fig. 4. The retention times of D,L-Trp were decreased with an increased in the ratio of MTMS (Fig. 5). The addition of MTMS to TMOS increased the enantioselectivity (α') and the values were 1.03 (0% MTMS), 1.13 (10% MTMS), and 1.05 (30% MTMS), respectively. However, 30% MTMS column was not stable in retention times and enantioselectivity. Taking into account the retention time and enantioselectivity, 10% MTMS was the best ratio.

To achieve the fast separation, buffer ionic strength for gel preparation was decreased from 50 to 20 mM, based on the study of Fig. 1B. Fig. 6 depicts the enantiomeric separation of D,L-Trp. Although the ionic strength was decreased, the retention times were almost the same as that in Fig. 5 (10% MTMS). The effect of the ionic strength was presumably negligible under the relatively high concentration of BSA. The enantioselectivity (α') was 1.10 and it was similar to that in Fig. 5 (10% MTMS, $\alpha' = 1.13$), which indicates that the effect of the ionic strength on the enantioselectivity was small.

3.3. Gel structure

In the process of the gelation, polycondensation of alkoxysilane monomers leads to the formation and growth of soluble particles and then colloids. These clusters coalesce and raise the solution

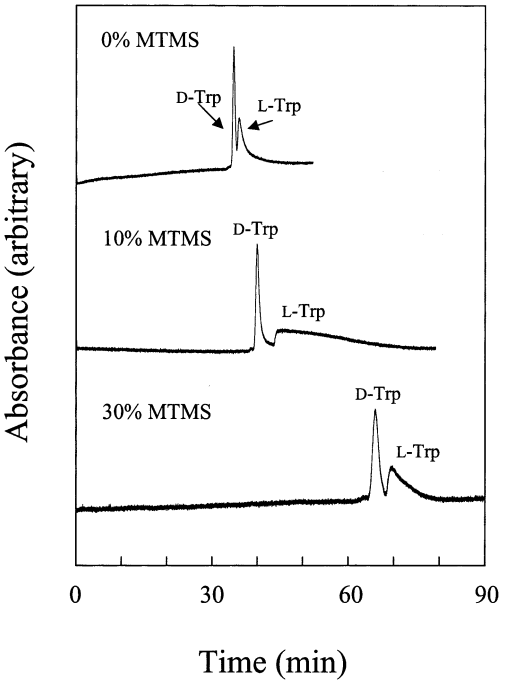

Fig. 5. Separation of D,L-Trp by BSA-encapsulated column prepared using different ratios of MTMS. *Conditions:* Gel composition: 5% (w/v) BSA in 50 mM phosphate buffer (pH 5): TMOS(containing 0–30% MTMS)-hydrolyed solution = 5:1. CEC conditions are the same in Fig. 4.

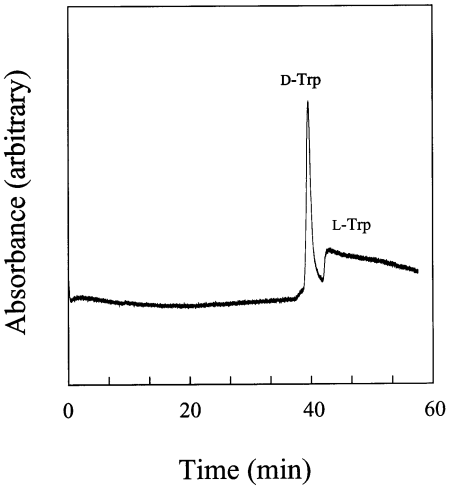

Fig. 6. Separation of D,L-Trp by BSA-encapsulated column prepared using 20 mM phosphate buffer (pH 5). *Conditions:* Gel composition: 5% (w/v) BSA in 20 mM phosphate buffer (pH 5): TMOS (containing 10% MTMS)-hydrolyzed solution = 5:1. CEC conditions are the same in Fig. 4.

viscosity to the sol–gel transition, at which bulk gelation occurs (gelation point) [19,23]. Because DLS is often used for measuring the hydrodynamic radius of macromolecule or colloid, the technique was employed to evaluate the changes in the cluster diameter during gelation process and investigate how proteins influence the gelation.

The cluster diameter was calculated from the light scattering intensity and the decay rate. Fig. 7 shows the time-dependent changes in the average diameter of clusters and the light scattering intensity during the gelation process. The strong fluctuation in the scattering intensity around 40 min shows the reaction reached the gelation point (Fig. 7) [24]. The diameter gradually increased and reached maximum around the gelation point. The maximum value was supposed to show the cluster diameter which constitutes bulk gel. Table 1 shows the average diameter of clusters, which constitute bulk gels. There was no significant difference between gels prepared with different compositions. These values are in good agreement with the values stated in the review by Gill and Ballesteros [23]. These results indicate that BSA does not largely influence the resultant gel state on a micro-scale.

Table 1
The average diameter of silica clusters

Gel	BSA[a]	No-BSA[b]	TMOS[c]
Average diameter (μm)	1.22	1.33	1.40

Gel composition.
[a] Gel composition, 5%(w/v) BSA in 50 mM phosphate buffer (pH 5.0): TMOS (containing 10% MTMS)-hydrolyzed solution = 5:1.
[b] 50 mM phosphate buffer (pH 5.0): TMOS (containing 10% MTMS)-hydrolyzed solution = 5:1.
[c] 50 mM phosphate buffer (pH 5.0): TMOS-hydrolyzed solution = 5:1.

3.4. Protein conformation before and after encapsulation in gels

IR spectra give a variety of information on the protein conformation [25]. The conformation of BSA in gel and in free solution was investigated using ATR-FT-IR. As illustrated in Fig. 8, two representative bands originated from BSA were observed in the region between 1800 and 1400 cm^{-1}. The signal around 1657 cm^{-1} is the amide I band, which mainly consists of $\upsilon_{C=O}$ stretching vibrations. The signal at 1549 cm^{-1} is the amide II

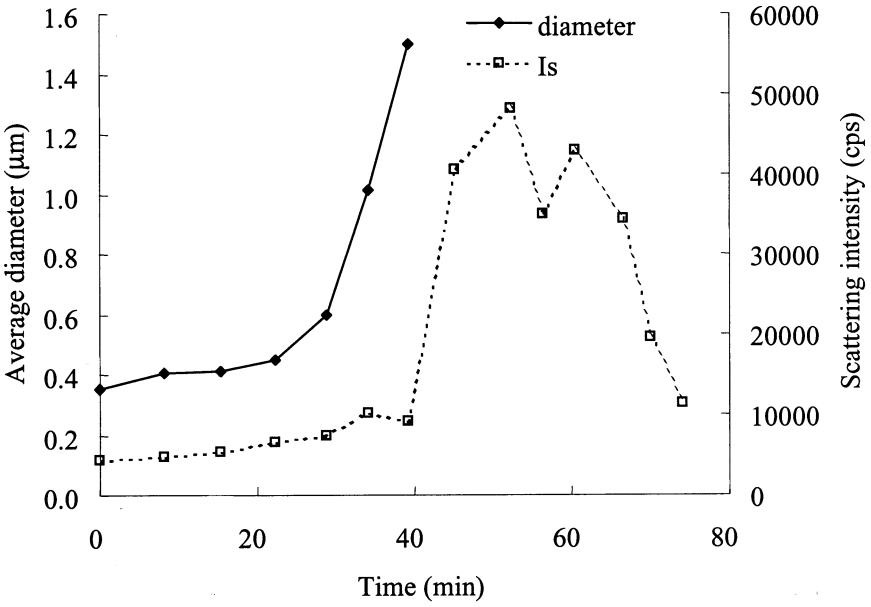

Fig. 7. Time-course of the average cluster diameter and scattering intensity (Is) during gelation process. Sample compositions: TMOS-hydrolyzed solution: 50 mM phosphate buffer (pH 5.0) = 1:5.

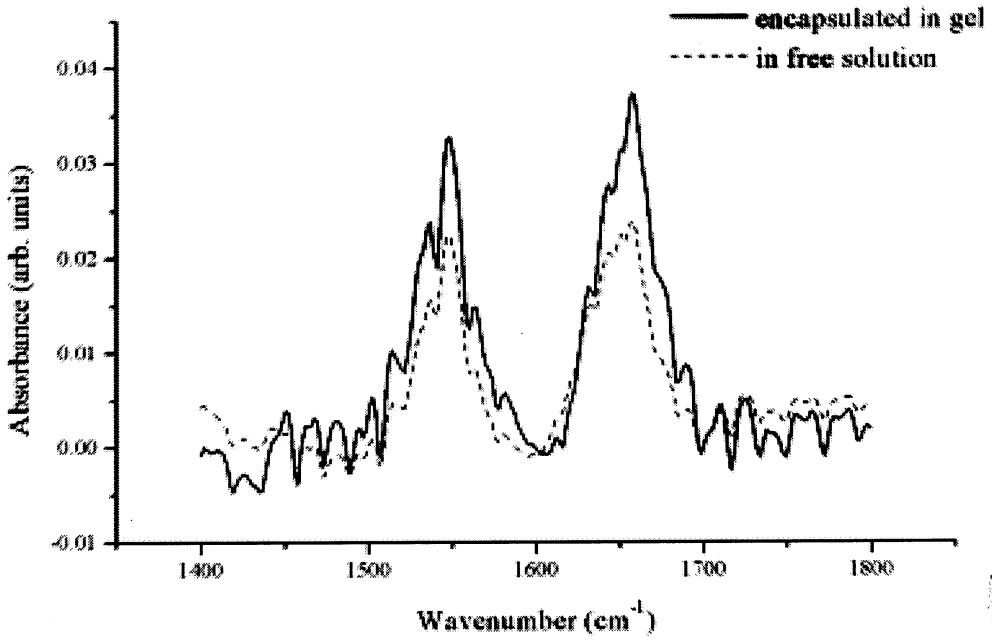

Fig. 8. IR spectra of BSA in gel or in free solution.

band, which mainly consists of υ_{N-H} bending vibrations. These two bands change its position depending on the structural changes as well as the degree of hydrogen bonding [18]. It is also reported that the amide I/amide II intensity and area ratios may be associated with conformational changes of the protein [18]. Table 2 shows the comparison of the peak positions and amide I/amide II area ratios obtained from BSA in gel and in free solution. The peak positions of each peak show no differences in both formats. Furthermore, the ratios of peak area are very close with each other. These strongly suggest that BSA maintain its conformation after encapsulation in the sol–gels.

The conformational stability of biomolecules is very important to maintain its biological activity. Silica hydrogels contain a sufficient amount of trapped interstitial water. Our hydrogel consist of about 80% water in their weight. Therefore the environment within hydrogel is essentially aqueous, allowing the retention of structure and reactivity of the encapsulated biomolecules. Our results support that this encapsulating technique is

Table 2
Comparison of the amide I and II bands for BSA encapsulated in gel or in free solution

	Position Amide I (cm^{-1})	Amide II (cm^{-1})	Area ratio (amide I/amide II)
Encapsulated in gel[a]	1657	1549	1.56
In free solution[b]	1657	1549	1.43

[a] Gel composition, 5%(w/v) BSA in 50 mM phosphate buffer (pH 5.0): TMOS (containing 10% MTMS)-hydrolyzed solution = 5:1.
[b] 5% (w/v) BSA in 50 mM phosphate buffer (pH 5.0).

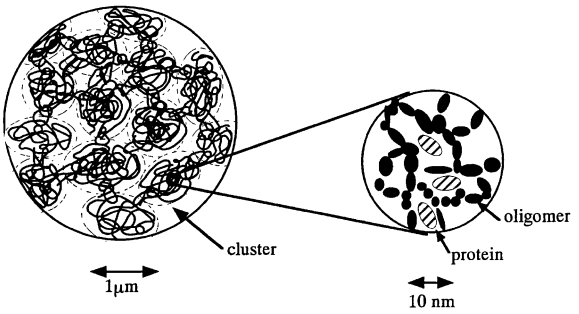

Fig. 9. Schematic diagram of sol–gel encapsulation of proteins.

very effective to make use of biomolecules in biological assay system.

Fig. 9 illustrates the schematics showing the macro- and micro-structures of the gel, taking account of our results and other reports [19,23,24,26–28]. The left diagram shows the magnified image of gel. Dot lines show the cluster unit and its diameter was about 1 μm. Each cluster is composed of silica networks which are depicted by the tangled lines. Some silica networks are formed between the clusters. The right diagram shows the magnified image of a part of the cluster. The closed circles are silica oligomers. The oligomers embed proteins during the cluster growth. The size of pores, where proteins are embedded, are reported to be 4–130 nm [23], which is suitable size for protein-encapsulation.

4. Conclusion

We developed a sol–gel method for preparation of protein-encapsulated monolithic columns for CEC. The monolithic packing was composed of TMOS-based hydrogel. Due to the silica-based matrix used, it is possible to control electroosmotic mobility by changing the gelation conditions such as buffer pH, ionic strength and starting materials. By using ATR-FT-IR, it was indicated that the electroosmotic mobility has close relationship with the contents of residual silanol groups in the gels. Enantiomeric separation of D,L-Trp was evaluated. Preparatory conditions for BSA-encapsulated columns also influenced the separation of D,L-Trp regarding the retention time and enantioselectivity. Based on the results, good enantioselectivity and stability of performance, such as retention times, was achieved.

As shown in our previous paper, this simple, in situ protein-encapsulating procedure is suitable for proteins to maintain their biological activity. This is also supported by the fact that BSA maintained its structure in gels under the optimized condition. The gel was formed from microclusters with the diameter of around 1 μm and BSA did not influence the value. The effect of gel structure on the chromatographic performances is further investigated in our laboratory.

Acknowledgements

This work was supported by a grant from Japan Health Sciences Foundation. The authors acknowledge Otsuka Electric Co. (Tokyo, Japan) for DLS measurements and JASCO Co. (Tokyo, Japan) for the useful advice on FT-IR measurement. The authors acknowledge Prof. K.K.-C. Yeung of the University of Western Ontario (Canada) for the useful comments on this work.

References

[1] V. Pretorius, B.J. Hopkins, J.D. Schieke, J. Chromatogr. 99 (1974) 23–30.
[2] J.H. Knox, I.H. Grant, Chromatogrphia 32 (1991) 317–328.
[3] S. Hjérten, Y.-M. Li, J.L. Liao, K. Nakazato, J. Mohammad, G. Pettersson, Nature 356 (1992) 810–811.
[4] F. Svec, J.M.J. Fréchet, Science 273 (1996) 205–211.
[5] H. Minakuchi, K. Nakanishi, N. Soga, N. Ishizuoka, N. Tanaka, Anal. Chem. 68 (1996) 3498–3501.
[6] M.T. Dulay, J.Q. Quirino, B.D. Bennett, M. Kato, R.N. Zare, Anal. Chem. 73 (2001) 3921–3926.
[7] M. Kato, K. Sakai-Kato, T. Toyo'oka, M.T. Dulay, J.Q. Quirino, B.D. Bennett, R.N. Zare, J. Chromatogr. A 961 (2002) 41–51.
[8] C. Fujimoto, Anal. Chem. 67 (1995) 2050–2053.
[9] C. Fujimoto, Y. Fujise, E. Matsuzawa, Anal. Chem. 68 (1996) 2753–2757.
[10] M. Kato, K. Sakai-Kato, N. Matsumoto, T. Toyo'oka, Anal. Chem. 74 (2002) 1915–1921.
[11] K. Sakai-Kato, M. Kato, T. Toyo'oka, Anal. Chem. 74 (2002) 2943–2949.

[12] K. Sakai-Kato, M. Kato, T. Toyo'oka, Anal. Biochem. 308 (2002) 278–284.
[13] M. Kato, N. Matsumoto, K. Sakai-Kato, T. Toyooka, J. Pharm. Biomed. Anal. 30 (2003) 1845–1850.
[14] Z. Chen, T. Hobo, Anal. Chem. 73 (2001) 3348–3357.
[15] J.R. Martínez, F. Ruiz, Y.V. Vorobiev, F. Pérez-Robles, J. González-Hernández, J. Chem. Phys. 109 (1998) 7511–7514.
[16] J.R. Martníez, F. Ruiz, J.A. De la Cruz-Mendoza, P. Villaseor-González, J. González-Hernández, M.M. González-Chávez, L. Valle-Aguilera, Revista Mexicana De Física 44 (1998) 575–579.
[17] R.J. Jakobsen, S.W. Strand, in: F.M. Mirabella, Jr. (Ed.), Internal reflection spectroscopy. Theory and applications Practical Spectroscopy Series, vol. 15, Dekker, New York, 1993, p. 107.
[18] C.E. Giacomelli, M.G.E.G. Bremer, W. Norde, J. Colloid Interface Sci. 220 (1999) 13–23.
[19] C.J. Brinker, G.W. Scherer, Sol–Gel Science: The physics and Chemistry of Sol–Gel Processing, Academic Press, New York, 1990.
[20] H.S. Dearie, V. Spikmans, N.W. Smith, F. Moffatt, S.A.C. Wren, K.P. Evans, J. Chromatogr. A 929 (2001) 123–131.
[21] L.A. Colón, Y. Guo, A. Fermier, Anal. Chem. (1997) 461A–467A.
[22] M. Cikalo, G. Bartle, K.D.M.M. Robson, P. Myers, M.R. Euerby, Analyst 123 (1998) 87R–102R.
[23] A. Gill, Ballesteros, Trends Biotechnol. 18 (2000) 282–296.
[24] T. Norisuye, M. Inoue, M. Shibayama, R. Tamaki, Y. Chujo, Macromolecules 33 (2000) 900–905.
[25] J. Gradadolnik, Y. Maréchal, Biopolymers 62 (2001) 40–53.
[26] L.M. Ellerby, C.R. Nishida, F. Nishida, S.A. Yamanaka, B. Dunn, J.S. Valentine, J.I. Sink, Science 255 (1992) 1113–1115.
[27] W. Jin, J.D. Brennan, Anal. Chim. Acta 461 (2002) 1–36.
[28] K. Ogino, Y. Osada, T. Hushimi, A. Yamauchi, Gel, Sangyo Tosho, Tokyo, 1998, pp. 3–5.